Current Science
CS 5 (2), 1536-1558 (2025)
Received 19 **Dec** 2024 | **Revised 23 Jan** 2025 | **Accepted 19 Feb**. 2025 | **Online Available 15 March** 2025
https://doi.org/ 10.52845/CS/2025-5-2-21

Current Science

Current Science

OPEN ACCESS

ISSN(O)2795-8639

ORIGINAL ARTICLE

Ribosome Biogenesis Related Genes as Prognostic Genes in Glioma: A Study Based on Transcriptomics and Mendelian Randomization

Yihong Chen

The First Affiliated Hospital, Sun Yat-Sen University

***Corresponding Author: Yihong Chen**

Abstract

Background: Ribosome biogenesis (RiboSis) is strongly associated with cancer progression, but its regulatory mechanisms in glioma are poorly understood. Therefore, it is of great significance to explore the relationship between ribosome biogenesis and glioma and to search for new prognostic genes for glioma.

Methods: Glioma related data and RBRGs were obtained from public databases and literature. Prognostic genes were obtained by differential expression analysis, Mendelian randomization (MR), as well as Cox and least absolute shrinkage and selection operator regression analysis (LASSO) regression analyses, and prognostic risk models were constructed and verified. The calculation of the risk groups score was the basis for the classification of glioma patients into high risk and low risk groups. Enrichment analysis, immune microenvironment analysis, drug sensitivity analysis and molecular docking were performed.

Results: Seven prognostic genes (NCL, FBLL1, YBEY, TP53, POP5, GNL2, and ZEB1) causally associated with glioma were obtained. The risk model effectively predicted the survival status of glioma patients. Enrichment analysis showed significant differences in pantothenate and CoA biosynthesis, and cardiac muscle contraction between high risk and low risk patients. Plasma B cells , monocytes, and activated natural killer (NK) cells were more abundant in the low risk groups. Conversely, M1/M2 macrophages and memory resting CD4+ T cells were more abundant in the high risk groups. Drug sensitivity analysis demonstrated that entrectinib and NVP-ADW742 exhibited the greatest discrepancy between the high-risk group and the low-risk group.

Conclusion: Seven prognostic genes, namely NCL, FBLL1, YBEY, TP53, POP5, GNL2, and ZEB1, were associated with RiboSis and effectively predicted survival in glioma patients, informing the development of more effective, individualized treatments.

Keywords: Glioma, Ribosome biogenesis, Prognostic risk model, Mendelian randomization, Immune microenvironment

Introduction

Glioma is one of the most common primary tumors of the central nervous system. And it is a heterogeneous tumor that ranges from a surgically curable low-grade glioma to a highly aggressive and virtually incurable glioblastoma multiforme. Although standard treatments such as surgery, radiation ,chemotherapy, Tumor treating fields or immunotherapy including immune checkpoint blockade, chimeric antigen receptor T (CAR T) cell therapy, oncolytic virotherapy, and vaccine therapy have increased in recent years, the prognosis for gliomas remains very pessimistic [1]. For patients with glioblastoma, even combination of temozolomide with radiotherapy can improved survival, the 5-year survival is still below 10%(9.8%)[2]; The median overall survival of Glioblastoma approximately 15 months[3]. Therefore, exploring the molecular mechanism of glioma is of great significance for improving treatment strategies and patient prognosis. The development of new prognostic models and personalized treatment plans will help improve the

accuracy and effectiveness of treatment.

The ribosome is an intercellular structure composed of proteins and nucleic acids and is responsible for protein synthesis in the cell[4]. Ribosome biogenesis (RiboSis) refers to the process of ribosome generation, which involves ribosomal RNA (rRNA) transcription, rRNA cleavage, rRNA modification, ribosome assembly, and the export of preribosomal particles. This process plays a crucial role in various cellular processes such as cell proliferation, differentiation, apoptosis, development, and transformation[5]. In malignant cells, somatic alterations occur in the genes involved in each substep of RiboSis, which will lead to an increased risk of ribosomosis and cancer[6]. Certain tumor suppressor genes and proto - oncogenes may regulate malignant progression by altering the protein synthesis machinery. The concept of "ribosome-transformed cancer" has gained increasing recognition[7].And the dysregulation of RiboSis in cancer cell proliferation provides a targetable weakness for cancer therapy[8]. Currently, RiboSis is still rarely mentioned in the treatment of glioma. Therefore, there is still a lot of room for the development of anti-tumor drugs targeting the RiboSis gene[9]. Determining the role of RiboSis in glioma may help develop better prognostic judgments and treatment strategies for glioma.

Mendelian randomization (MR) is a powerful genetic technique that uses genetic variants as instrumental variables (IVs) to evaluate the potential causal relationship between the exposure factors under study and the target outcomes[10]. Compared with traditional observational studies, Mendelian randomization has the advantages of avoiding the influence of environmental confounding factors and excluding reverse causal relationships[11]. In the research of glioma, Mendelian randomization has been used to explore the potential relationships between factors such as the duration of telephone use[12] , viral infections[13], mental disorders[14], etc., and glioma.

Our study, based on the transcriptome of public databases and combined with MR analysis, identified the prognostic genes associated with RiboSis in glioma, constructed a prognostic risk model to predict the survival of glioma patients, and explored a series of biological functions of the high and low risk groups, so as to provide a new reference for the clinical prognosis prediction and immunotherapy of glioma.

2. Materials and Methods

2.1 Data Collection

The data of 638 glioma tissue samples with their RNA-seq, survival information, clinicopathological parameters and somatic mutation data were obtained from The Cancer Genome Atlas (TCGA) database (https://portal.gdc.cancer.gov/) and defined the training set TCGA-GBM/LGG in this study (visit time: Sep 20, 2024). GSE16011 (GPL2567) dataset, including 276 glioma tissue samples and 8 normal tissue samples from the Gene Expression Omnibus (GEO) database (https://www.ncbi.nlm.nih.gov/geo/), was used for differential expression analysis. Additionally, CGGA-mRNAseq_325 dataset as validation set, comprising 325 glioma tissue samples, was obtained from the Chinese Glioma Genome Atlas (CCGA) database (http://www.cgga.org.cn). In addition, 331 ribosome biogenesis (RiboSis) related genes (RBRGs) were obtained from the literature (**Supplementary Table 1**) [6].

2.2 Differential Expression Analysis and Enrichment Analysis

To identify differentially expressed genes (DEGs), in GSE16011 dataset, the “limma” package (v 3.54.0)[15] was used to perform differential expression analysis on glioma and normal samples ($|\log_2$ fold change (FC)$| > 0.5$, $P < 0.05$). For visualization, “ggplot2” package (v 3.5.0)[16] and “ggrepel” package (v 0.9.5)[16] were used to plot the volcano plot, and “ComplexHeatmap” package (v 2.18.0) [17] were used to plot the heatmap, respectively. Subsequently, Gene Ontology (GO) and Kyoto Encyclopedia of Genes and Genomes (KEGG) analysis were conducted in order to ascertain the potential biological functions and mechanisms of the DEGs utilising the “clusterProfiler” package (v 4.10.1) ($P < 0.05$)[18].

2.3 Identification of the Candidate Genes

To identify candidate genes, “ggvenn” package (v 0.1.10)[19] was used to obtain the intersection genes between DEGs and RBRGs. Subsequently, pathways for candidate genes enrichment were analyzed using the Metascape database

(http://metascape.org). Continually, protein protein interaction (PPI) network was plotted by using Search Tool for the Retrieval of Interacting Genes/Proteins database (STRING, https://string-db.org/) and drawn with Cytoscape software (v 3.10.2)[20]. It was recommended that a minimum interaction score of 0.4 be set as a prerequisite for protein-protein interaction (PPI) analysis.

2.4 Screening of Instrumental Variables (IVs)

The finn-b-C3_GBM_EXALLC also was obtained through the Integrative Epidemiology Unit Open genome-wide association study (IEU OpenGWAS) database (https://gwas.mrcieu.ac.uk/) database, consisting of 16,380,303 single nucleotide polymorphisms (SNPs) in 174,097 European samples (glioma: 91 and normal samples: 174,006). The IVs were then screened using the extract_instruments function from the "TwoSampleMR" (v 0.6.4)[21]. Here were the criteria for filtering IVs: (1) SNPs that exhibited a strong correlation with exposure factors were selected as IVs ($P < 5\times10^{-8}$); (2) Linkage disequilibrium (LD) IVs need to be excluded using clumping = TRUE, $r^2 < 0.001$, and kb = 10; (3) The weak IVs with F-statistics value < 10 were removed; (4) Based on the outcome GWAS data, as well as the IVs from the previous screening, IVs significantly correlated with the outcome were removed.

2.5 Mendelian Randomization (MR) Analysis

There were three major assumptions in MR analysis: (1) the hypothesis proposed a significant association between IVs and exposure variables; (2) the independence assumption: there was independence between IVs and confounders; (3) the exclusivity assumption: the IVs can only has an effect on the outcome through the exposure factor. Effect alleles and effect sizes were aligned using the harmonise_data function from the "TwoSampleMR" package (v 0.6.4). MR methods included MR-Egger [22], Weighted median[23], Inverse variance weighted (IVW) [24], Simple mode [21] and Weighted mode [25]. The most important of these methods was IVW. Exposure factors with $P < 0.05$ in IVW were selected as candidate exposure factors of potential relevance. The findings were visually represented using scatter plots to illustrate individual associations, forest plots that consolidated effect sizes along with their confidence intervals, and funnel plots to evaluate the presence of any potential publication bias and heterogeneity amongst the results. In addition, a sensitivity analysis was carried out to assess the confidence in the results of the MR analysis. The MR_heterogeneity function in "TwoSampleMR" package (v 0.6.4) was analyzed for heterogeneity, and $P > 0.05$ suggested the absence of heterogeneity. The horizontal pleiotropy test was then executed utilizing the "TwoSampleMR" package (v 0.6.4) mr_pleiotropy_test function, and $P > 0.05$ indicating that there were no confounders. The leave-one-out (LOO) analysis was carried out utilizing the "TwoSampleMR" package (v 0.6.4) mr_leaveoneout function, where each SNP was systematically excluded to assess its impact on the remaining SNPs on the results. Finally, the Steiger directional test was applied to eliminate the prospect of reverse causation. The evidence of a one-way causal association was strengthened when the correct_causal_direction outcome was confirmed as TRUE and the steiger_pval was < 0.05. In particular, genes that passed the Steiger directionality test were used for subsequent analyses and were selected as MR genes.

2.6 Prognostic Genes Identification and Genemania Network Construction

To investigate the correlation between MR genes and overall survival (OS) in glioma patients, we conducted a univariate Cox regression analysis (hazard ratio (HR) $\neq 1$, $P < 0.05$) by "survival" package (v 3.5-3) [26] and performed a proportional hazards (PH) assumption test ($P > 0.05$) to screen for prognostic related genes. The result was visualized via "forestplot" package (v 3.1.1)[27]. Further, the "glmnet" package (v 4.1-4) [28] was used to carry out least absolute shrinkage and selection operator regression analysis (LASSO) regression analysis, and the best lambda-value was determined by 10-fold cross-validation to screen for prognostically related genes. Finally, prognostic genes were found using multivariate Cox regression analysis (HR $\neq 1$, $P < 0.05$) with the "survival" package (v 3.5-3) and the PH assumption test ($P > 0.05$).

2.7 Construction and Validation of a Prognostic Risk Model

In the TCGA-GBM/LGG dataset, a prognostic genes-based risk model was constructed using the following formula:

Risk Score = $\sum_{i=1}^{n}$Coefficient$_i$ × Gene Expression Level$_i$

The Coefficient and Expression Level represents the risk coefficient and expression of each gene, respectively. The glioma samples with survival information were classified into high and low risk groups based on optimal cutoff value for the risk score. A Kaplan-Meier (KM) curve was generated using the "survminer" package (v 0.4.9) [29] to analyse the difference in OS between two risk groups. The log-rank test was used to assess the significance of these survival differences with $P < 0.05$. Furthermore, receiver operating characteristic (ROC) curve was generated using the "survival ROC" package (v 1.0.3)[30] to assess the prognostic efficacy by calculating the area under the curve (AUC). Furthermore, an additional assessment was conducted to evaluate the accuracy and generalisability of the prognostic risk model, which was validated in the CGGA-mRNAseq_325 dataset..

2.8 GeneMANIA Network and Gene Set Enrichment Analysis (GSEA)

To predict the function of the prognostic genes and to discover novel gene associations, GeneMANIA (http://genemania.org/search/) was used to create a gene-gene interaction networks to assess genes function.

In an effort to find some relevant pathways and biological mechanisms between two risk groups, "DESeq2" (v 1.38.0) [31] package was employed to perform the deviation analysis of two risk groups in the TCGA-GBM/LGG dataset. Then, $\log_2$FC values of genes were sorted from largest to smallest. GSEA was performed via "clusterProfiler" package (v 4.2.2)[32] (|normalized enrichment score (NES)| > 1, $P < 0.05$, false discovery rate (FDR) < 0.2). The reference gene set employed was "c2.cp.kegg. v7.5.1. symbols.gmt" from the Molecular Signatures Database (MSigDB, https://www.gsea-msigdb.org/gsea/msigdb/). The "psych" package (v 2.1.6) [33] was employed to ascertain the intercorrelations between the risk score and enrichment pathways (|correlation (r)| > 0.3, $P < 0.05$).

2.9 Mutation analysis

The TCGA-Glioma somatic mutation information was downloaded using the "TCGAmutations" package (v 0.4.0)[34] and analyzed to identify non-synonymous somatic mutations. Moreover, the tumour mutation burden (TMB) was calculated based on somatic nonsynonymous mutations, and "maftools" package (v 2.18.0) [35] was ploted the waterfall plot. The TMB difference of two risk groups was assessed by Wilcoxon test ($P < 0.05$). The optimal TMB cutoff value was calculated using the "survival" package (v 3.5-3), after which the glioma patients in the TCGA-GBM/LGG were divided into low and high TMB groups. Subsequently, we conducted a Kaplan-Meier analysis to ascertain any differences in OS between the two groups. Similarly, in order to evaluate the mixing functions of riskscore and TMB, the glioma patients were divided into four groups according to both TMB and riskscore. Subsequently, a comparison of OS was conducted across the four groups

2.10 Antitumor Immune Response

The Cancer-Immunity Cycle comprises seven steps. It begins with the release of antigens and continues with presentation, priming, trafficking, infiltration, T-cell recognition and killing. The genes associated with the Cancer-Immunity Cycle were sourced from the Tumor Immunophenotype (TIP) website (http://biocc.hrbmu.edu.cn/TIP/), and scored using the ssGSEA algorithm with the "GSVA" package (v 1.50.5) [36]. The Cancer-Immunity Cycle score difference of two risk groups was compared by Wilcoxon test ($P < 0.05$).

2.11 Immune Characteristic Analysis

The relative infiltration levels of 22 types of immune cells[37] were quantified using the CIBERSORT algorithm in the TCGA-GBM/LGG dataset. Furthermore, the discrepancy in the proportions of immune cells between the risk groups was evaluated using the Wilcoxon test ($P < 0.05$). A total of eight immune checkpoint-related genes were identified through a review of the relevant literature[38]. The expression differences of immune checkpoint related genes in two risk groups was assessed by a Wilcoxon test with a significance level of $P < 0.05$. Furthermore, a number of additional signatures were gathered, which delineated specific features of immunity. The aforementioned signatures encompassed the single-cell state, the tumour microenvironment and immunotherapy. Further detailed information regarding these signatures could be found in **Supplementary Table 2**. The ssGSEA algorithm

calculated the score of there related genes using the "GSVA" package (v 1.50.5), the Wilcoxon test was compared the score difference between samples from high and low risk ($P < 0.05$), and Spearman correlation analysis of risk score and signatures score was used "psych" package (v 2.2.9) ($|r| > 0.3$ and $P < 0.05$).

2.12 Drug sensitivity Analysis

Drug sensitivity data from the Genomics of Drug Sensitivity in Cancer (GDSC) database (https://www.cancerrxgene.org/) were used to assess chemotherapy response in glioma patients in the TCGA-GBM/LGG Half-maximal inhibitory concentration (IC50) values of glioma samples were estimated via "oncoPredict" package (v 0.1) [39]. Drugs were screened by Spearman correlation analysis of IC50 correlation with risk score using the "psych" package (v 2.2.9) ($|r| > 0.3$ and $P < 0.05$). The IC50 of two risk groups was evaluated using the Wilcoxon test with a significance level of $P < 0.05$ and visualized by the "ggplot2" package (v 3.5.1).

2.13 Molecular Docking

The 3D structures of proteins (prognostic genes) and molecular ligands (predicting drugs with the highest differential expression) were obtained from the Protein Data Bank (PDB) database (https://www.uniprot.org/) and PubChem database (https://pubchem.ncbi.nlm.nih.gov/), respectively. Then the proteins and ligands were uploaded to the PyMOL software (v 3.0.3) (https://pymol.org/) for molecular docking and their binding free energies were calculated.

2.14 Statistical Analysis

The Wilcoxon test was employed to ascertain whether there were notable statistical differences between the risk groups, with a P of less than 0.05 deemed to be statistically significant. The R programming language (v 4.2.2) was employed for the purposes of bioinformatics.

3. Results

3.1 Strong associations between 109 candidate genes with both glioma and RiboSis

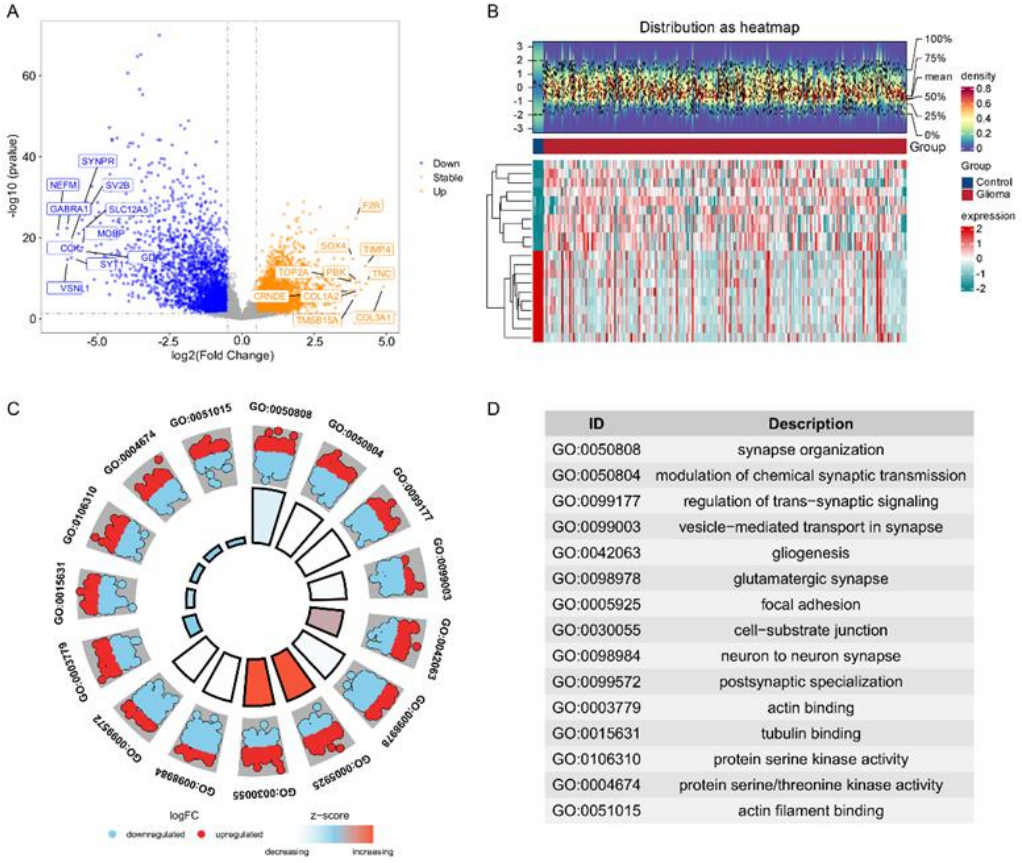

ID	Description
GO:0050808	synapse organization
GO:0050804	modulation of chemical synaptic transmission
GO:0099177	regulation of trans−synaptic signaling
GO:0099003	vesicle−mediated transport in synapse
GO:0042063	gliogenesis
GO:0098978	glutamatergic synapse
GO:0005925	focal adhesion
GO:0030055	cell−substrate junction
GO:0098984	neuron to neuron synapse
GO:0099572	postsynaptic specialization
GO:0003779	actin binding
GO:0015631	tubulin binding
GO:0106310	protein serine kinase activity
GO:0004674	protein serine/threonine kinase activity
GO:0051015	actin filament binding

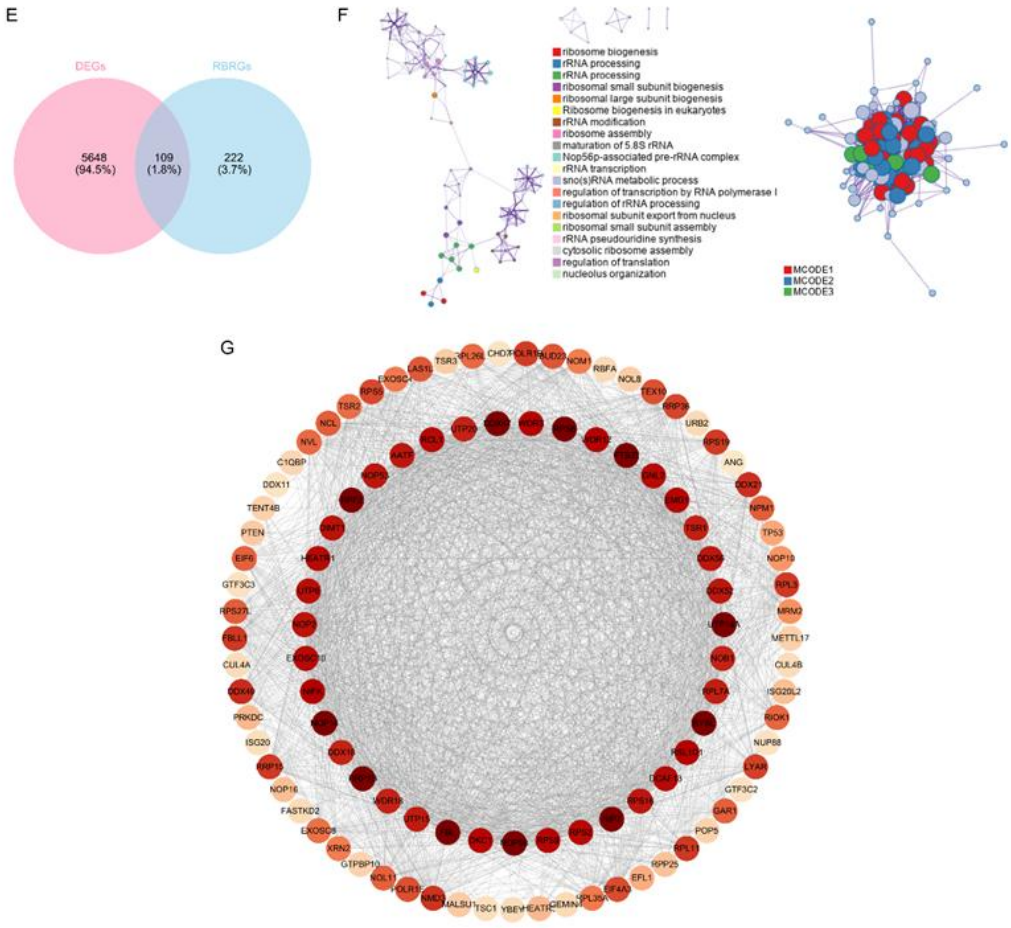

Figure 1 ***Analysis of genes related to glioma. Volcano plot of upregulated/downregulated genes (A). Heatmap of the top 10 upregulated/downregulated genes (B). Results of GO analysis (C). Pathways enriched by differentially expressed genes (D). Candidate genes associated with both glioma and RBRGs (E). Biological functions enriched by candidate genes (F). Interactions among candidate genes (G).***

Differential expression analysis between the glioma tissue samples and normal tissue samples revealed 5,757 DEGs, including 3,272 up- and 2,485 down-regulation genes. The volcano plot marking the top 10 up/down genes was shown in **Figure 1A**. Besides, the heatmap of the top10 up/down genes was shown in **Figure 1B**. The GO analysis results showed a significant enrichment in the 1,791 different entries. Among them, 1,444 biological processes (BP) like modulation of chemical synaptic transmission were enriched, 244 cellular components (CC) like neuron to neuron synapse were enriched and 103 molecular functions (MF) like protein serine kinase activity were enriched (**Figure 1C**). Besides, KEGG pathway enrichment significantly enriched were a total of 104 pathways like proteoglycans in cancer, MAPK signaling pathway, AGE-RAGE signaling pathway in diabetic complications, GABAergic synapse, and cellular senescence (**Figure 1D**). Further, DEGs and RBRGs were investigated to discover 109 candidate genes that were linked with both glioma and RBRGs (**Figure 1E**). Metascape analysis revealed enrichment of candidate genes to ribosome biogenesis, rRNA processing, rRNA modification, and so forth (**Figure 1F**). These results indicated that candidate genes were mainly associated with these pathways, which aided in understanding the potential roles of RBRGs in glioma. Furthermore, a PPI network of candidate genes was constructed, which shown interaction between 104 genes except NUDT16, RBIS, SPIN1, NSUN5P1 and NSUN5P2 (**Figure 1G**). The PPI network uncovered the intricate interactions among these genes, underscoring their possible importance in glioma progression.

3.2 Identification of 35 MR genes causally associated with glioma in MR analysis

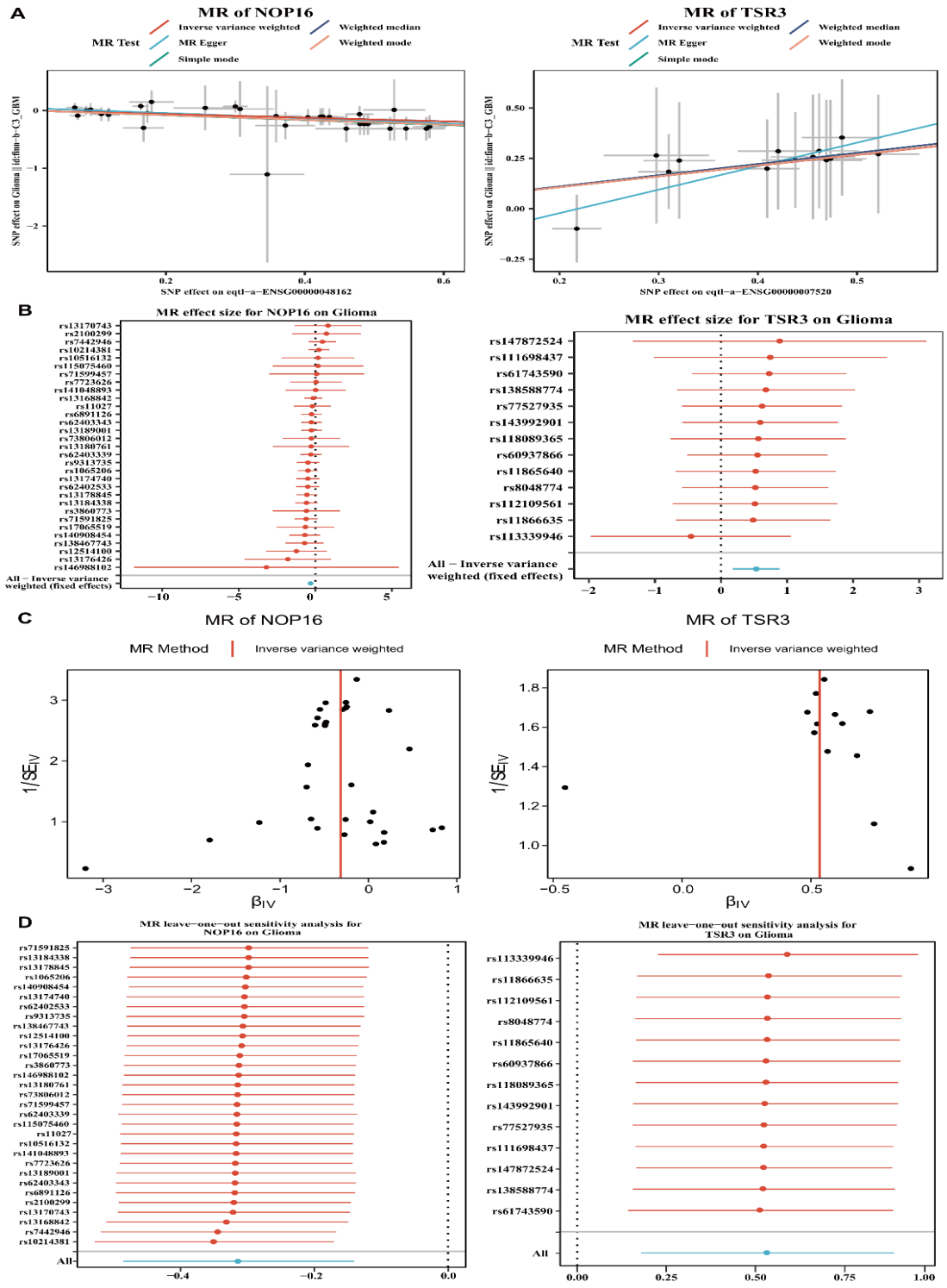

Figure 2 Mendelian randomization (MR) analysis, with candidate genes as exposure factors and glioma as the outcome indicator. Risk factors and protective factors (A). The forest plot shows the significant effect of the IVW model (B). The funnel plot indicates that the selected instrumental variables (IVs) conform to Mendel's second law (C). The results remain unchanged after eliminating each SNP (D).

A MR analysis was executed by acquisition of expression quantitative trait loci (eQTL) data for 106 candidate genes, which were used as exposure factors, and glioma, which was used as an outcome. As a result, NOP14, DDX56, EXOSC8, RRP1B, NOL8, BUD23, POLR1B and UTP6 were heavily influenced by confounding factors and were excluded, in total 35 MR genes were

causally associated with glioma **(Supplementary Table 3)**. The results showed that there were 17 risk factors (e.g. TSR3) (OR > 1, P < 0.05 in IVW) and 18 protective factors (e.g. NOP16) (OR < 1, P < 0.05 in IVW) (**Figure 2A, Supplementary Figure 1)**. The forest plots demonstrated a significant effect of the IVW model, specifically, the forest plots showed the IVW value (fixed effects > 0) was less than zero of 18 protective factors (e.g. NOP16), and IVW value (fixed effects < 0) was more than zero of 17 risk factors (e.g. TSR3) (**Figure 2B, Supplementary Figure 2)**. The funnel plots showed the SNPs for the 35 candidate exposure factors were distributed to a large extent symmetrically and homogeneous in number, it showed that the selected IVs conformed to Mendel's second law (e.g. NOP16 and TSR3) (**Figure 2C, Supplementary Figure 3**). P values in heterogeneity test for 35 candidate exposure factors exceeded 0.05, indicating no heterogeneity **(Supplementary Table 4)**. In horizontal pleiotropy test, 35 candidate exposure factors also exceeded 0.05 **(Supplementary Table 5)**. After each SNP was gradually eliminated, the impact of the remaining SNPs on the outcome variables remained largely unchanged, suggesting the MR analysis results were reliable (e.g. NOP16 and TSR3) **(Figure 2D, Supplementary Figure 3)**. Notably, the Steiger directional test showed that the direction of all 35 candidate exposure factors mentioned above was TRUE (P < 0.05), indicating a correct causal relationship among exposure factors and outcome **(Supplementary Table 6)**. Therefore, 35 MR genes causally associated with glioma were used for subsequent analyses.

3.3 Model construction and evaluation of prognostic risk Score

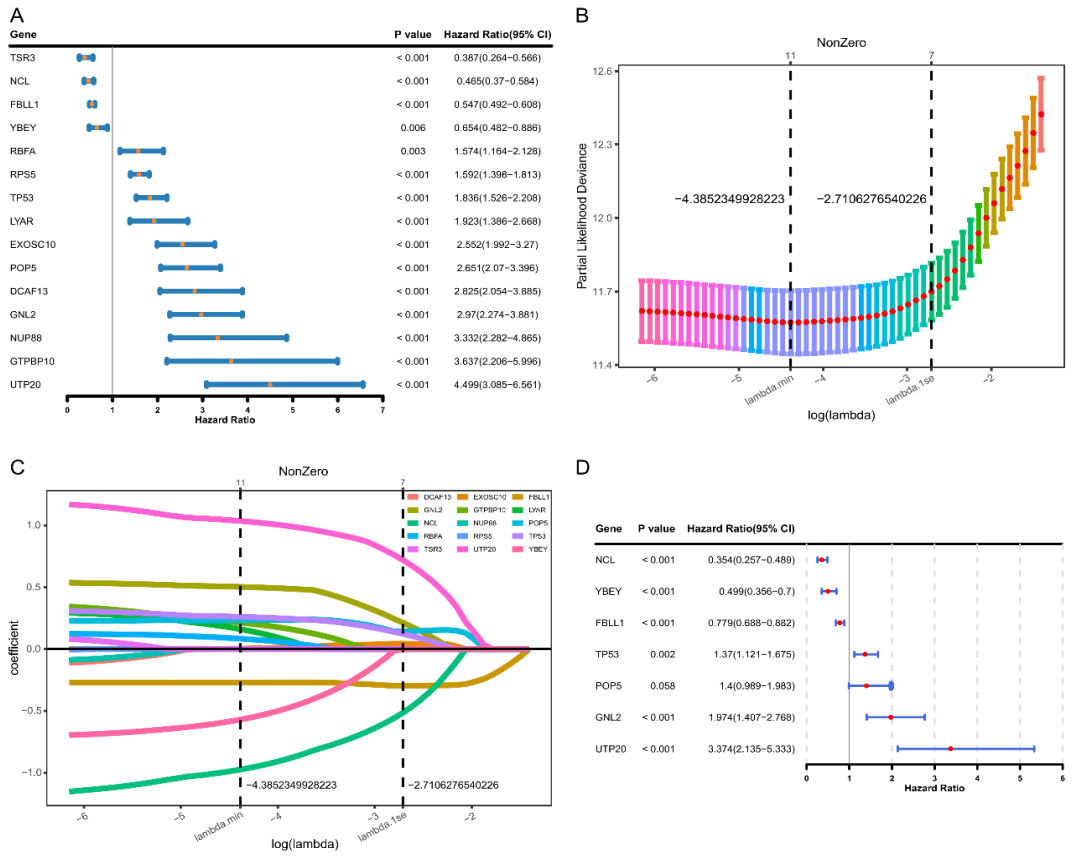

Figure 3 7 prognosis - related genes were selected. 3 genes are associated with a better prognosis, and 4 genes are associated with a poor prognosis.

Following the univariate/univariate Cox regression analysis and LASSO regression analysis (optimal lambdamin = 0.03129353), seven prognostic genes were selected (**Supplementary Table 7-8, Figure 3A-3D**). NCL, FBLL1 and YBEY were associated with a better prognosis (HR < 1), while TP53, POP5, GNL2, and UTP20 were associated with a poor prognosis (HR > 1).

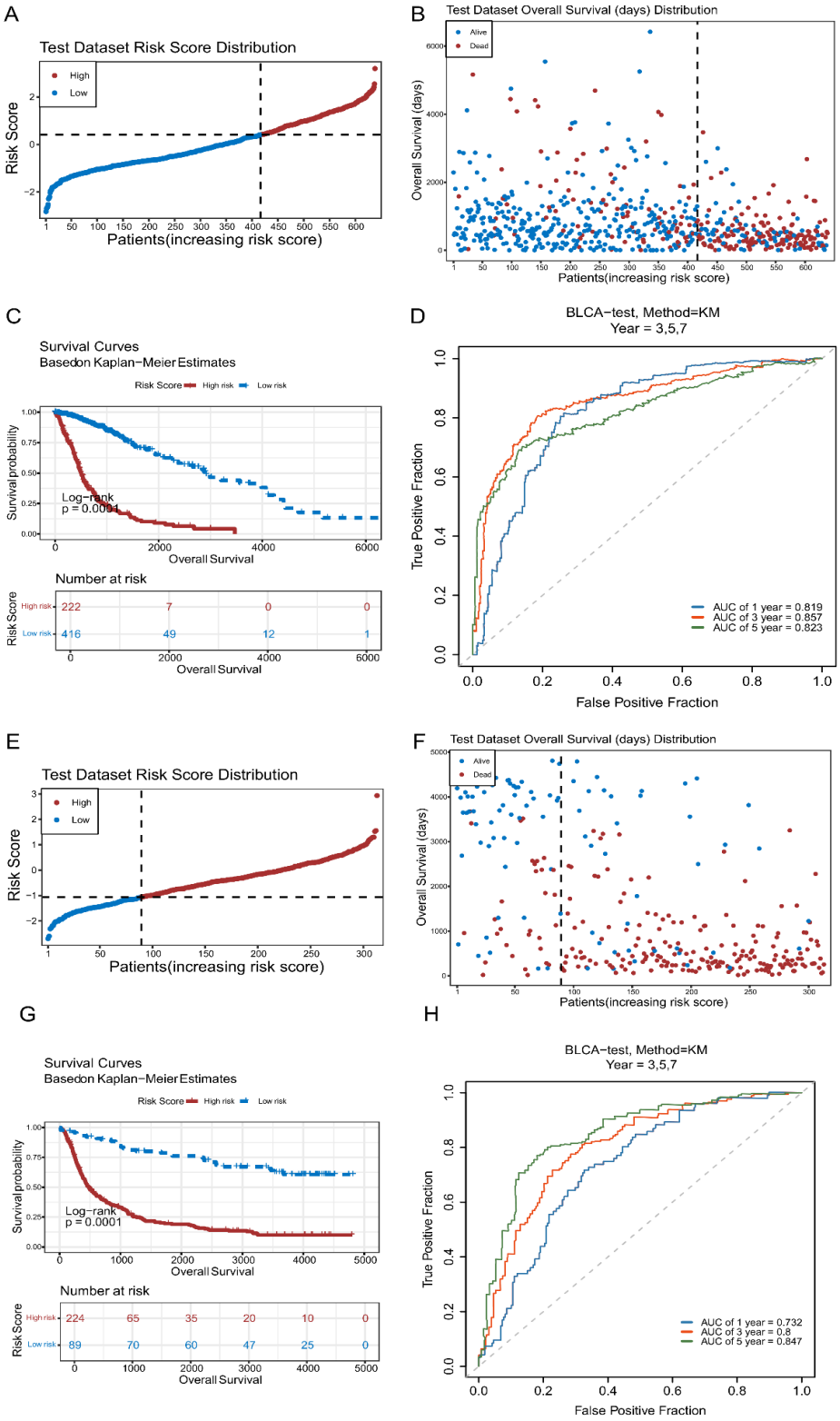

Figure 4 Establishment of a risk model. Grouping based on risk scores (A). The mortality rate of glioma patients is positively correlated with the risk score (B). The survival rate of the high - risk group is lower than that of the low - risk group (C). The AUC value of the risk model (D). Validation of the risk model using public databases (E - F). The prognosis of high - risk patients is worse than that of low - risk patients (G - H).

The glioma samples were categorised as high risk (222 glioma patients) and low risk (416 glioma patients) by best cutoff value for the risk score of 0.4122488. It was noteworthy that the mortality

rate of glioma patients in TCGA increased in a progressive manner with increasing risk scores (**Figure 4A-4B**). The high risk exhibited a poorer survival rate than the low risk, with $P < 0.05$ (**Figure 4C**). The ROC results (AUC > 0.6) indicated that the risk model could make good predictions for the survival of glioma patients (1-, 3-, 5-year survival with AUC value of 0.819, 0.857, 0.823) (**Figure 4D**).

In order to provide further validation of the robustness of the risk model, the glioma samples in CGGA-mRNAseq_325 were classified into a high risk (comprising 224 individuals) and a low risk (comprising 89 individuals) by best cutoff value for the risk score of -1.066821. The mortality rate of glioma patients increased progressively with increasing risk scores (**Figure 4E-4F**). The results demonstrated that high risk patients exhibited inferior outcomes in comparison to low risk patients ($P < 0.05$) (**Figure 4G**). The 1-, 3-, 5-year survival with AUC value were 0.732, 0.8, and 0.847 (**Figure 4H**), respectively, which were all > 0.6, demonstrating that the risk model had a certain degree of robustness.

3.4 GeneMANIA Network and Risk Subtype Enrichment Analysis

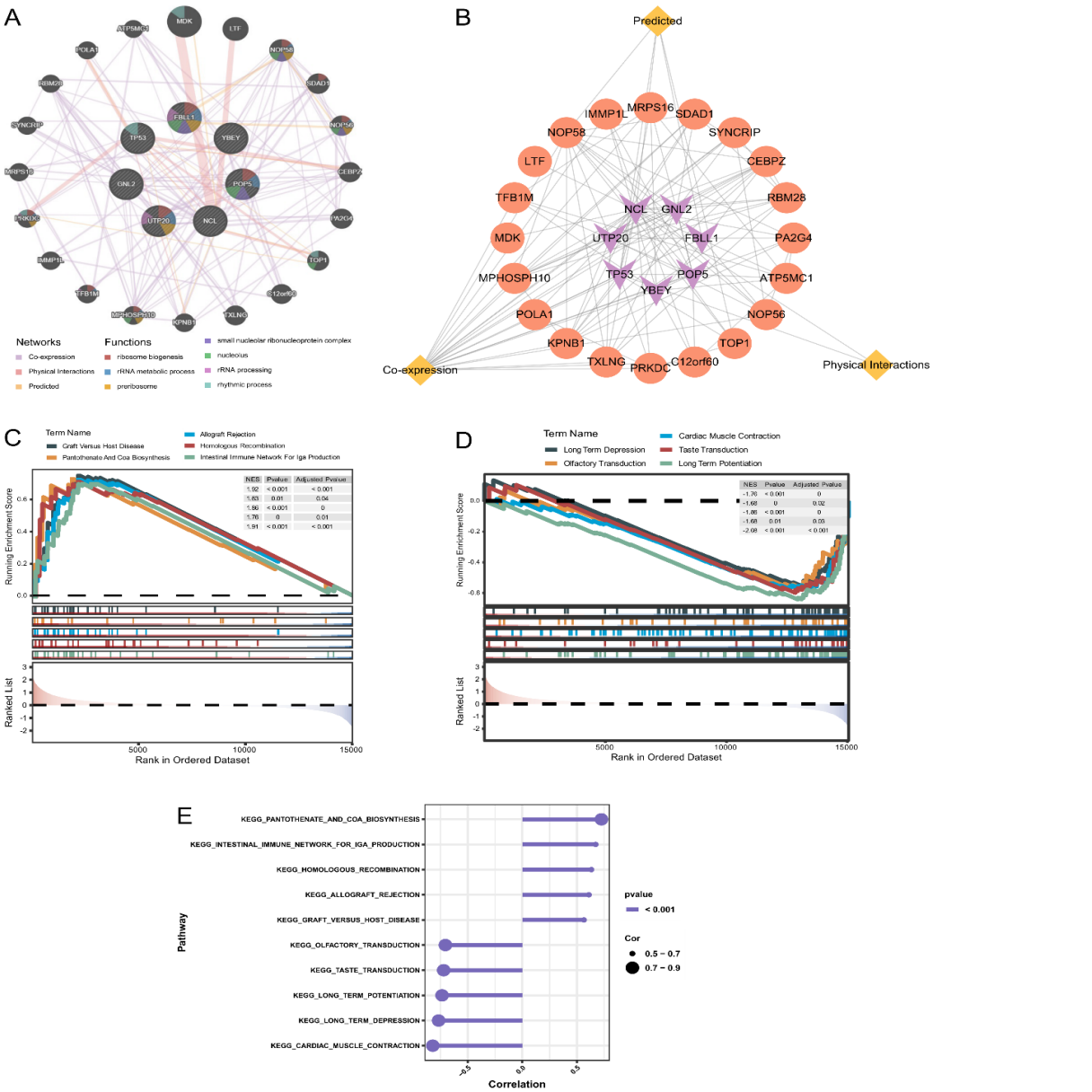

Figure 5 Gene - gene interaction network of prognostic genes. The interrelationships and related functions of prognostic genes (A - B). Pathways enriched in the high - risk group and pathways enriched in the [It seems there is a mistake here, should it be "low - risk group"?] risk group (C - D). These pathways are significantly correlated with the risk score (E).

Gene-gene interaction network was built for the prognostic genes using the GeneMANIA database in order to investigate the potential functions of these genes. Twenty nodes of genes that were significantly enriched for prognostic genes circled the hub node representing prognostic genes (**Figure 5A**). Their functions focused on ribosome biogenesis, rRNA metabolic process and rhythmic process. NCL-LTF/MDK in physical interaction, FBLL1-NOP56/58 in prediction and NCL-PA2G4/ADAD1/SYNCRIP in co-expression were strongly linked (**Figure 5B**).

A GSEA analysis revealed that 53 pathways were enriched between the high and low risk. Graft-versus-host disease, pantothenate and CoA biosynthesis, allograft rejection, homologous recombination, and intestinal immune network for IgA production were enriched in the high risk (**Figure 5C**). Long term depression, olfactory transduction, cardiac muscle contraction, taste transduction, and long term potentiation were enriched in the low risk (**Figure 5D**). The above pathways were significantly associated with the risk score, with all absolute values of correlation greater than 0.5 and P less than 0.001 (**Figure 5E**).

3.5 Tumor Mutational Burden (TMB)

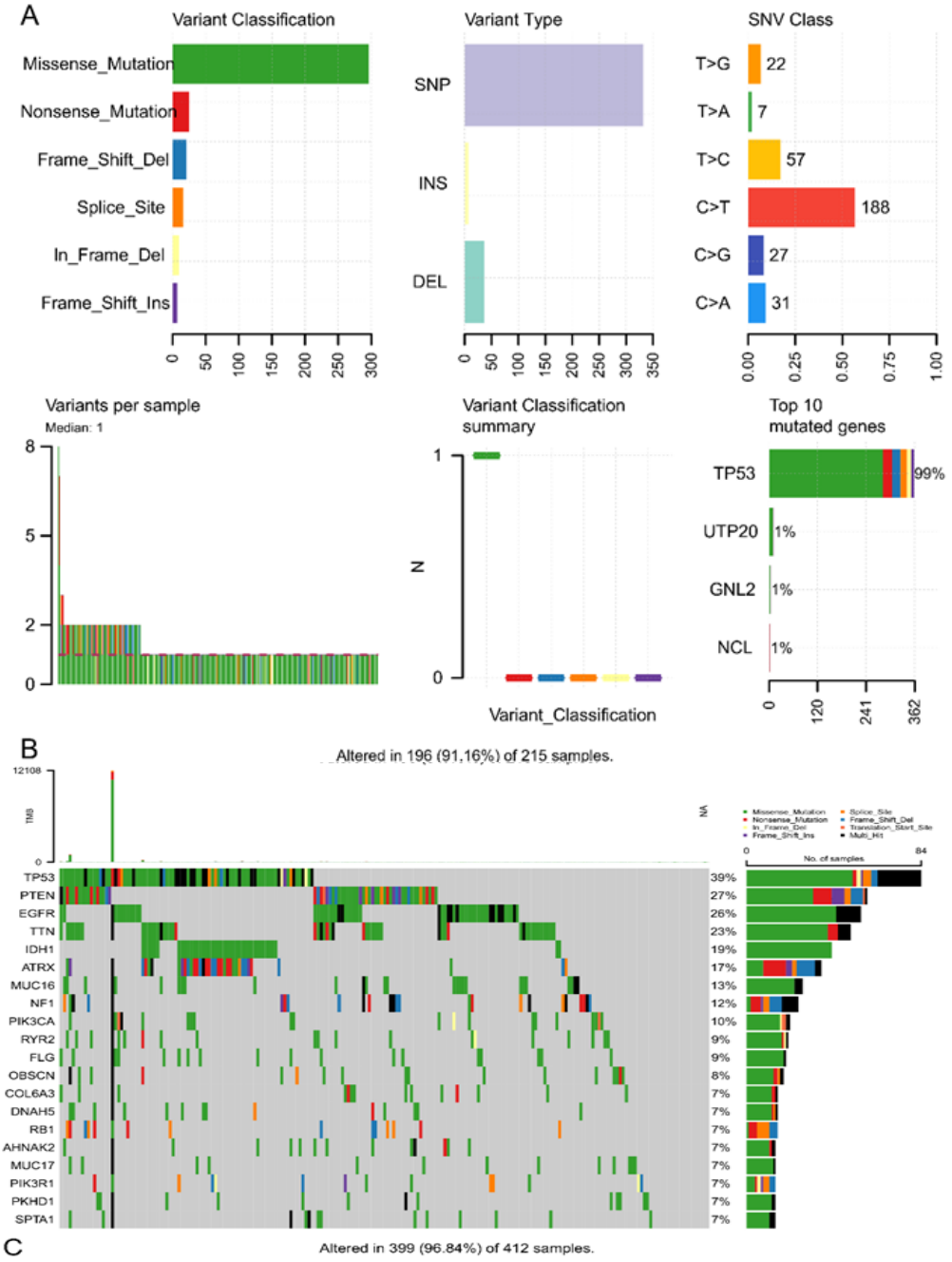

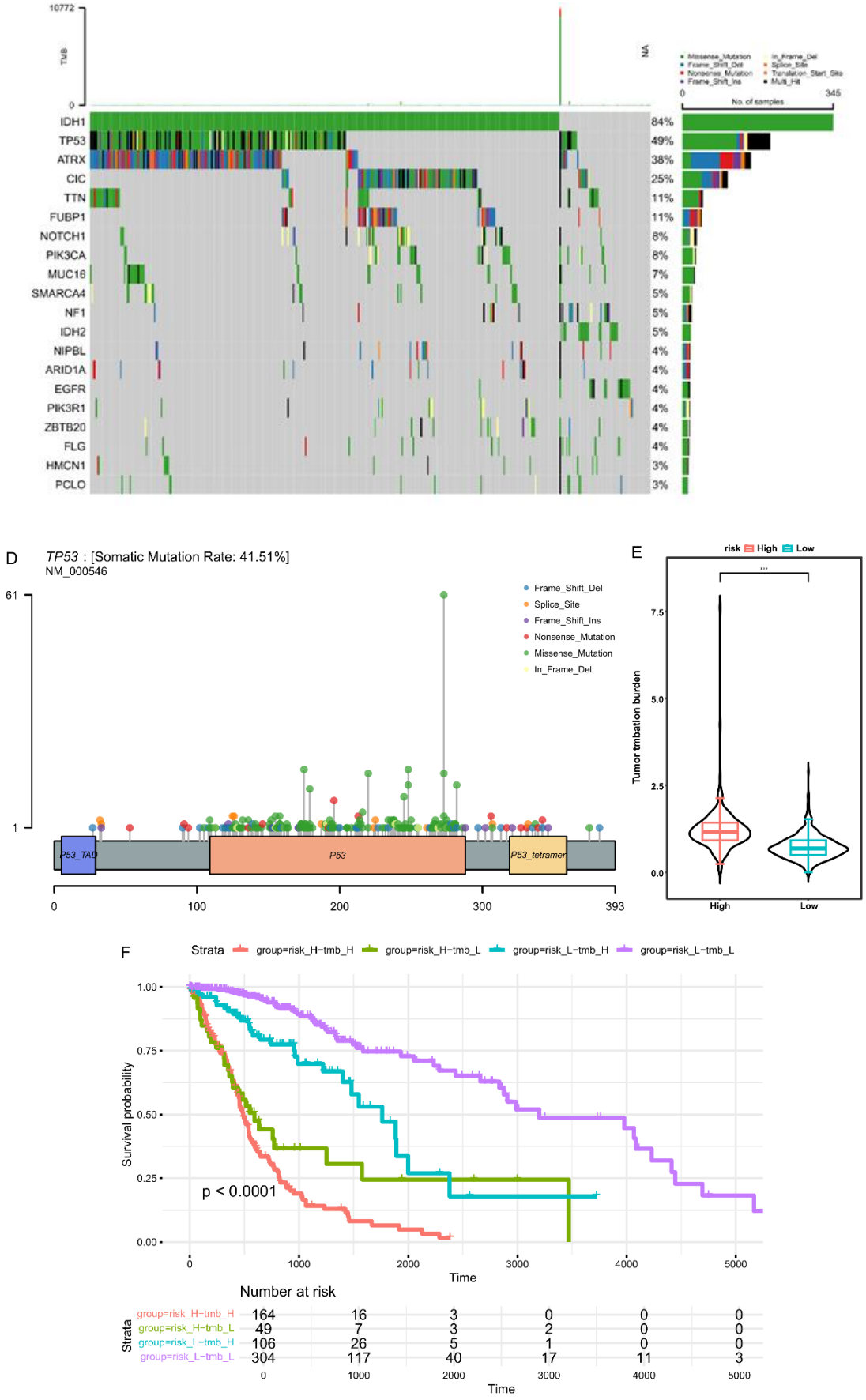

Figure 6 Gene mutations in glioma. Proportions of different gene mutations (A). IDH1 and TP53 genes are the most common mutations (B - C). The mutation type and mutation location of TP53 (D). Relationship among high - risk score, tumor mutational burden and prognosis (E - F).

Genetic alterations also exert a substantial influence on the processes of tumorigenesis and prognosis. Missense mutations were the most common in patients with glioma, single nucleotide polymorphisms appeared more commonly as insertions or deletions, and C > T was the most frequent single nucleotide variation (SNV) (**Figure 6A**). The top 20 genes alterations were illustrated in waterfall maps, delineating the genetic profiles of two groups. The most common alterations seen in the high risk and low risk groups were in the IDH1 and TP53 genes, respectively (**Figure 6B-6C**). However, the mutation type and mutation location of TP53 were different (**Figure 6D**). Additionally, we confirmed that there was more TMB accumulated in the high risk ($P < 0.001$) **(Figure 6E)**. Furthermore, survival analysis demonstrated that glioma patients with elevated TMB and high risk were linked to a poor prognosis ($P < 0.0001$) **(Figure 6F)**.

3.6 Differential Immune Microenvironment and Immunotherapy Responses

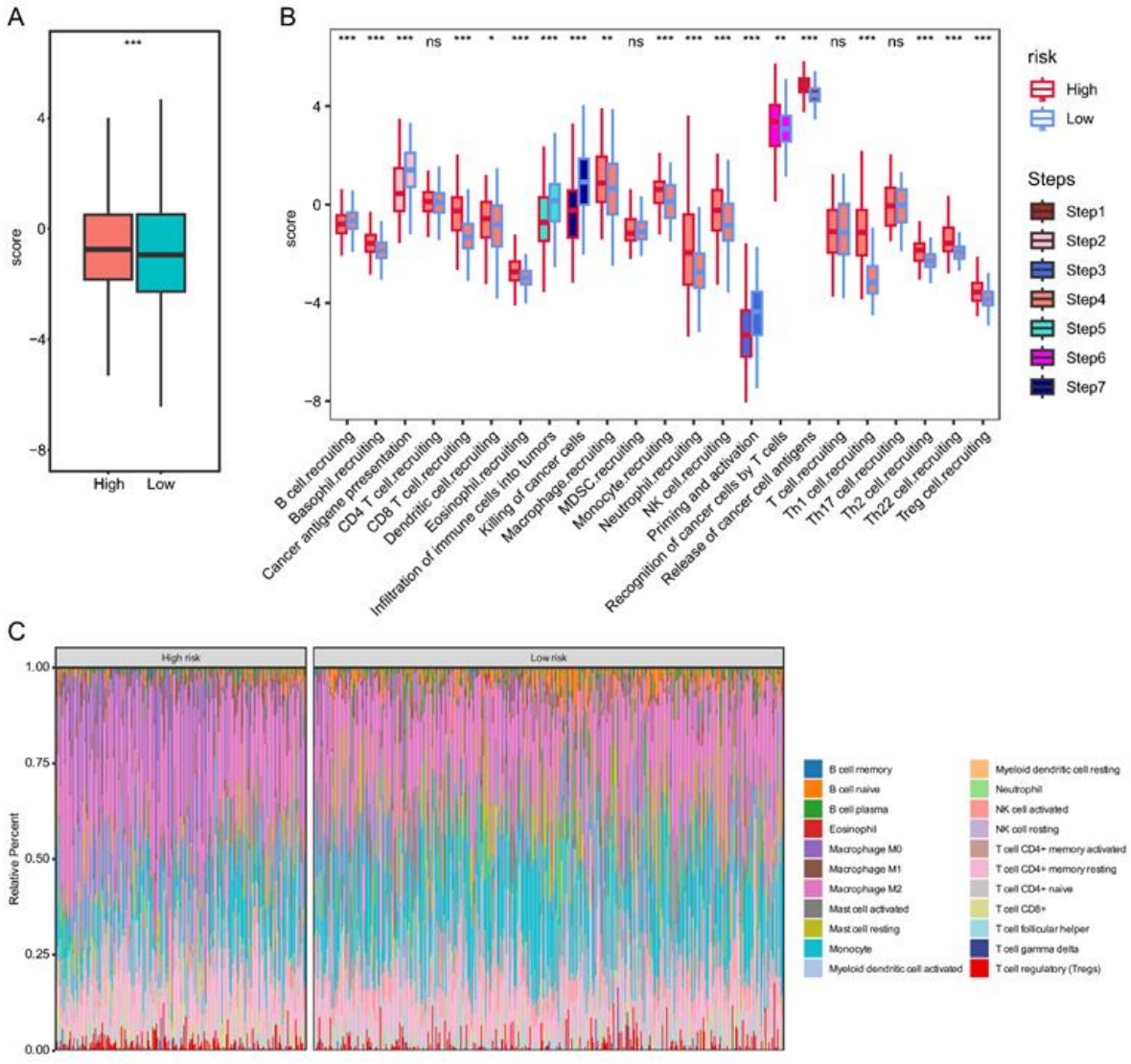

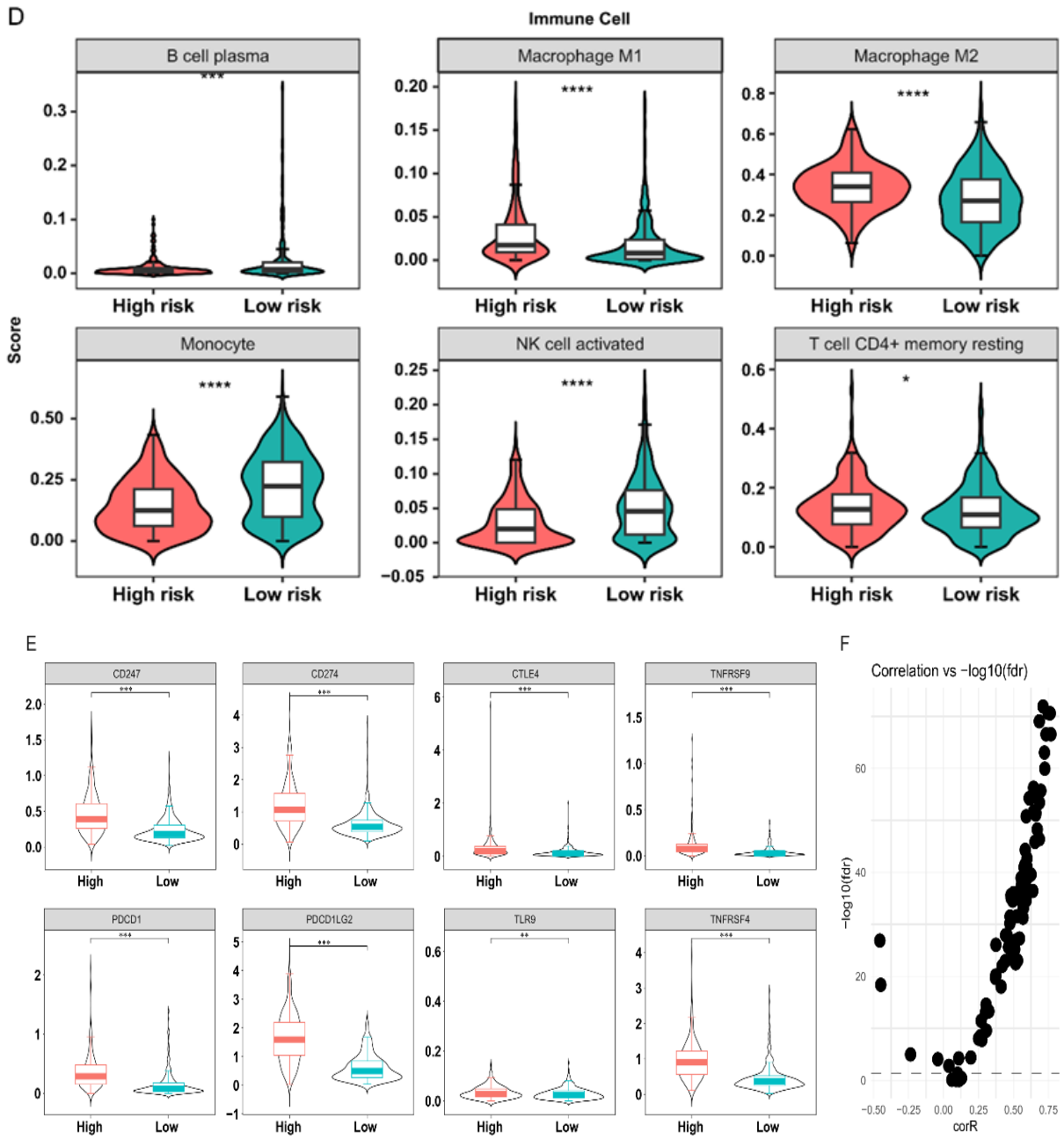

Figure 7 Signatures of the anti-tumour immune cycle at high risk. The high-risk group has a stronger anti-tumour immune response (A). Most immune cells in the high-risk group have stronger migration ability (B). Differences in the proportion of immune cells (C - D). Differences in the expression of immune checkpoint-related genes (E). Most immune-related scores are positively correlated with the risk score (F).

Signatures of the anti-tumour immune cycle were elevated in individuals at high risk, suggesting that the anti-tumour immune response was activated ($P < 0.001$) (**Figure 7A**). The high risk demonstrated a greater capacity to release cancer antigens in comparison to the low risk. In regard to the trafficking of cells, the trafficking abilities of Th22 cells, dendritic cells, eosinophils, macrophages, monocytes, neutrophils, natural killer (NK) cells, Th1 cells, Th2 cells, CD8 T cells and Treg cells were more capable in the high-risk group, while B cells demonstrated greater capability in the low-risk group (**Figure 7B**). The ratio of 22 immune cells in the individual specimens was determined (**Figure 7C**). Among these, three types immune cells, including plasma B cells , monocytes, and activated NK cells, exhibited significantly higher levels of invasion in low risk. Conversely, three types of immune cells,

including M1 macrophages, M2 macrophages, and memory resting CD4+ T cells showed markedly greater levels of invasion in the high risk ($P < 0.05$) (**Figure 7D**). Additionally, expressions of eight immune checkpoints-related genes like TNFRSF9, CD247, PDCD1LG2, PDCD1, CTLA4, TNFRSF4, TLR9 and CD274 of two groups were significantly differed ($P < 0.01$) (**Figure 7E**). Correlations between a series of immune-related scores and the aforementioned risk score were calculated, and the results demonstrated a positive correlation between the majority of immune-related scores and the risk score ($|r| > 0.3$, $P < 0.05$) (**Figure 7F**).

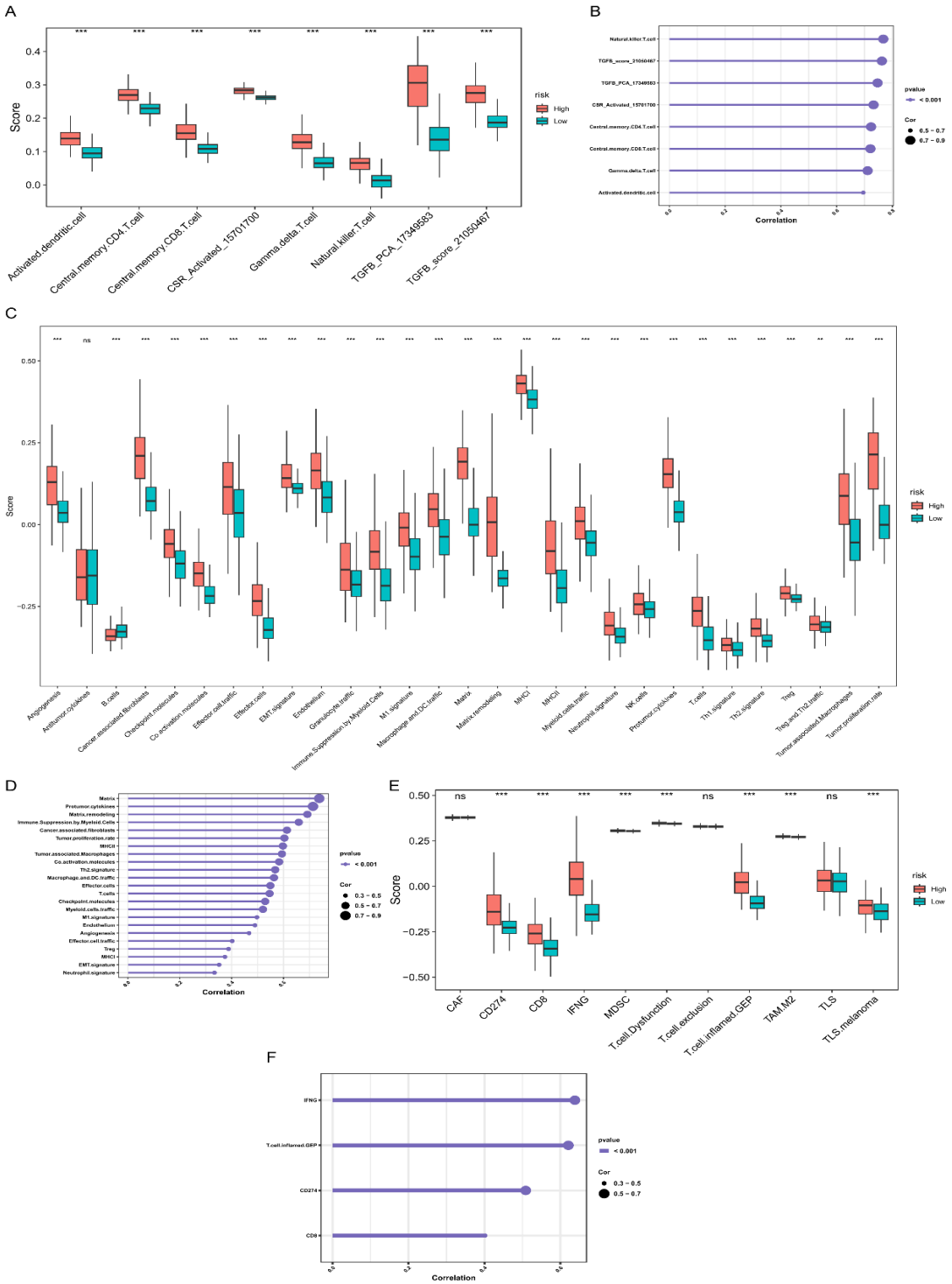

Figure 8 Anti - tumour immune response at high risk. Factors promoting the malignant progression of tumors are at higher levels in high - risk individuals, and they are all positively correlated with the risk score (A - D). Characteristics related to the immunotherapy response are significantly correlated with the risk score (E - F).

The GSVA results demonstrated that factors facilitating the aggressive advancement of tumours, including natural killer T cells, TGFB score 21050467, matrix, protumour cytokines, matrix remodelling and immune suppression by myeloid cells, were significantly higher in the high risk than in the low risk ($P < 0.001$) (**Figure 8A, 8C**), and they were all positively correlated risk score ($r > 0.3$, $P < 0.001$) (**Figure 8B, 8D**). In order to examine this phenomenon, a number of signatures associated with immunotherapy response were assembled, revealing that the risk score exhibited a positive correlation with the GSVA scores of the aforementioned signatures (IFNG, inflamed T cell, GEP, CD274 and CD8) ($r > 0.3$, $P < 0.001$) (**Figure 8E**), and all varied significantly in the high risk ($P < 0.001$) (**Figure 8F**). The study findings indicate that patients with an elevated risk may derive greater benefit from immunotherapy than those with a lower risk.

3.7 Drug Sensitivity Analysis and Target-Medicine Interaction

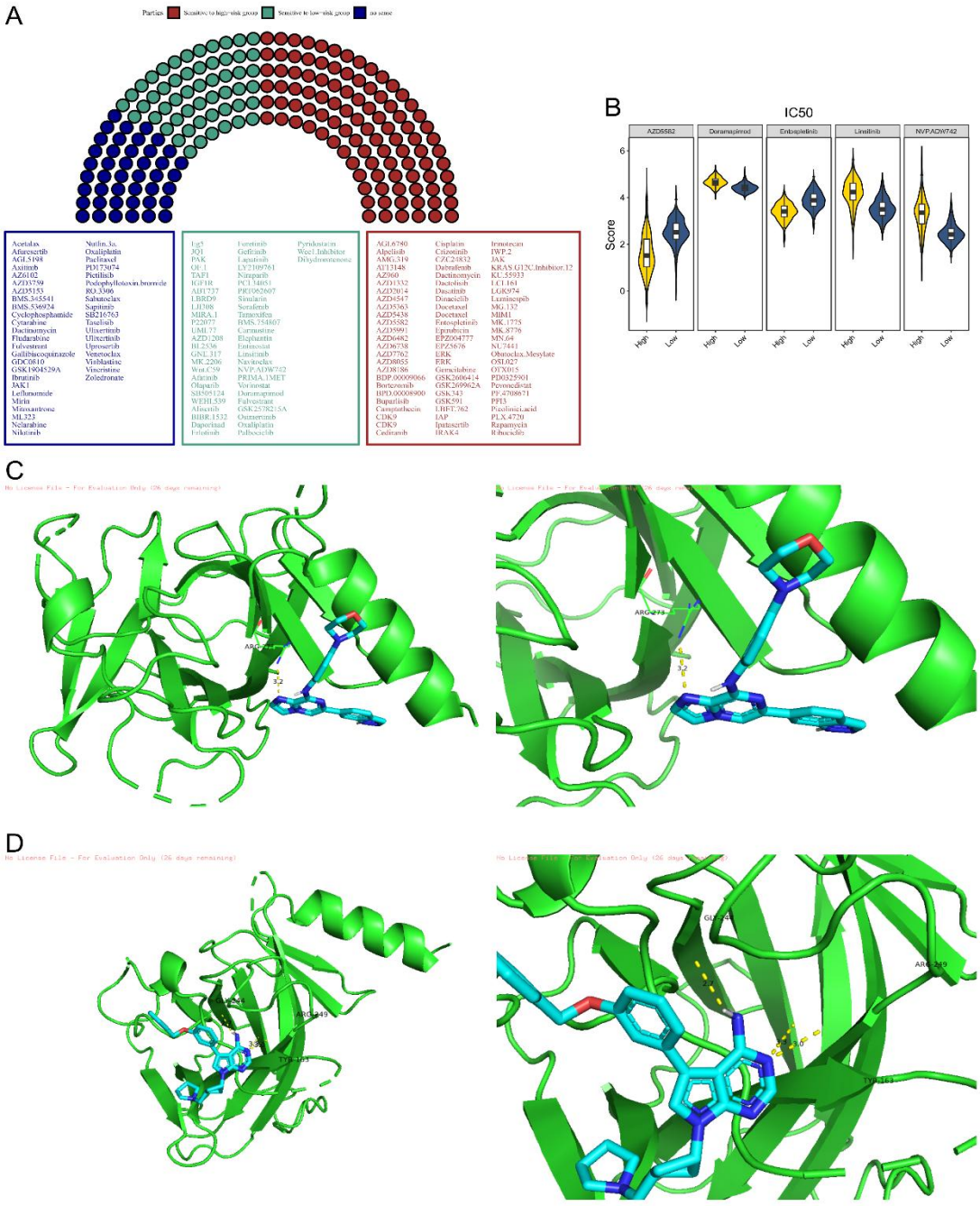

Figure 9 Analysis of drug sensitivity. Association between risk score and anti - tumor drug sensitivity (A). Differences in anti - tumor drug sensitivity between the two groups (B). Drug molecular docking analysis (C - D).

The study further analyzed the GDSC databases to determine the association between risk score and antineoplastic drug sensitivity of glioma patients (**Figure 9A**). A total of 102 drugs in the high risk showed significant associations and 53 drugs in the low risk ($|r| > 0.3$, $P < 0.001$) (**Supplementary Table 9**). Further analysis showed that AZD5582, and entospletinib were more sensitive in high risk patient, instead, doramapimod, linsitinib and NVP-ADW742 were more sensitive in low risk patients (**Figure 9B**). Among them, entospletinib and NVP-ADW742 showed the highest difference in the two groups ($P < 0.001$).

To further explore the role of TP53, the prognostic gene with the highest mutation rate, the drug with the highest 2D conformation score of entospletinib and NVP-ADW742 was selected for molecular docking (**Figure 9C-9D**). The results showed the binding energy of TP53 to entospletinib was -7.0 kcal/mol, and that of TP53 to NVP-ADW742 was -7.2 kcal/mol.

4. Discussion

Glioma is a tumor that originates from glial cells in the nervous system and is the most common intracranial malignancy, accounting for about 30% of the total number of intracranial tumors. Ribosome biogenesis refers to the process of ribosome formation and maturation, which includes multiple steps such as the synthesis and modification of ribosomal RNA (rRNA) and the assembly of proteins. In cancer cells, genes involved in ribosome production are often mutated, increasing the risk of cancer[40]. For the crucial role of ribosome biogenesis in cancer development, it is of great significance to understand its relationship with glioma. Our study , which was based on the transcriptome datasets in the GEO, TCGA and CGGA databases, combined with MR analysis identified the prognostic genes associated with RiboSis in glioma, constructed a prognostic model, and explored its potential molecular regulatory mechanisms. Thereby, it provides scientific references and new targets for the prognostic diagnosis and immunotherapeutic approaches of glioma.

Our study identified 7 prognostic genes for ribosome production that regulate glioma progression. Based on the existing literature and our analysis results, seven prognostic genes and their risk models (NCL, FBLL1, YBEY, TP53, POP5, GNL2, and UTP20) are discussed.

NCL (nucleolin) is one of the most abundant proteins in the nucleolus and plays a central role in polymerase I transcription. NCL is also found in the nucleoplasm, cytoplasm, and cell membrane. On cell membranes, NCL have been found to interact with several ligands involved in cell proliferation, apoptosis, and angiogenesis. Previous studies have shown that NCL is mainly lactylated at lysine 477 by the acyltransferase P300 in response to excessive glycolytic activity, which promotes the proliferation and invasion of intrahepatic cholangiocarcinoma (iCCA) cells[41]. Some research has found that compared with normal human astrocytes (NHA), NCL is overexpressed in the nucleus and cytoplasm of human glioma U87, U251 and SHG44 cells. The binding of NCL to AS1411 can inhibit the proliferation of glioma cells, but not that of NHA[42]. Other studies have indicated that the novel inhibitor of histone acetyltransferases (INHAT) repressor activates rDNA transcription through the cooperation of two important nucleolar transcription factors, NCL and nucleophosmin 1 (NPM1), to promote the proliferation of glioma stem cells[43].

FBLL1(Fibulin 1) is a secreted glycoprotein that becomes incorporated into a fibrillar extracellular matrix. FBLL1 is a key snoRNP complex enzyme that transfers methyl groups to substrate RNAs both in vitro and in vivo. FBLL1 is preferentially expressed in the brain, especially in human neuron cells, and promotes neuronal differentiation through 2'-O-methylation of GAP43 messenger RNA (mRNA). Knocking down FBLL1 ultimately leads to the inhibition of neuronal differentiation [44].

YBEY (UPF0054 family protein YbeY) is implicated in ribosomal maturation and quality control and plays a particularly important role in the regulation of small subunit biogenesis and post-transcriptional gene expression. Deletion of YBEY is often fatal or associated with severe alterations in cellular metabolism and growth. Some studies have shown that YBEY is significantly correlated with the missense variant C21orf58 in breast cancer. This suggests that YBEY may have a functional role in the growth of tumor cells[45].

The TP53 gene is a major contributor to cancer

formation and is considered to be the most important tumor suppressor gene. The p53 protein is a transcription factor involved in DNA repair, senescence, cell cycle control, autophagy, and apoptosis. In addition to cancer, there is evidence that TP53 is also associated with fertility, aging, and longevity. In addition, genetic variants in TP53 are associated with environmental adaptation. The characteristic mutations of TP53 are quite common in gliomas. Previous studies have shown that TP53 mutations have a high incidence in low-grade astrocytomas and secondary glioblastoma multiforme (GBM). Low-grade gliomas with TP53 mutations have a poorer prognosis[46].

POP5 is a subunit of the RNase P/MRP complex. Previous studies in S. cerevisiae have shown that specific components of the homologous complex play a role in the regulation of telomerase holoenzyme complexes. In addition, POP1, another subunit of the RNase P/MRP complex, has also recently been shown to interact with human telomerase RNA60, and POP protein also plays a role in human telomerase regulation. Previous studies have shown that the overexpression of the POP5 gene can lengthen telomeres. This suggests that the POP5 gene may be associated with the transformation of normal cells into tumor cells with the ability of unlimited proliferation[47].

GNL2 is a nucleolar guanosine triphosphate-binding protein. It interacts with the 60S ribosomal subunit in the nucleus and then shuttles to the cytoplasm, participating in the nuclear export process of ribosomal subunits. The rapid proliferation of tumor cells requires a large amount of proteins, which depends on efficient ribosomal biosynthesis. By promoting the transportation of ribosomal subunits, GNL2 ensures that there are sufficient ribosomes in the cytoplasm for protein synthesis, thus providing a material basis for the proliferation of tumor cells. In hepatocellular carcinoma, the expression of GNL2 is mostly increased, and its over expression is closely related to different stages of the cancer and poor prognosis. Since ribosome biogenesis plays a crucial role in the unrestricted growth of tumor cells, and GNL2 is involved in the transportation of ribosomal subunits, it is speculated that it may promote the proliferation, migration, and invasion of tumor cells by affecting ribosome biogenesis[48].

UTP20: t-UTP is required for the early stages of PolI transcription and pre-rRNA processing, and previous studies identified 1A6/DRIM as human UTP20, primarily playing a role in 18S rRNA processing. Related reviews have shown that the upregulation of UTP20 is associated with various cellular biological processes such as cell cycle progression, proliferation, migration, and invasion. It plays a crucial role in the tumorigenesis of multiple cancer types, including breast cancer, colon cancer, lung cancer, gastric cancer, and adult T-cell leukemia[49].

Based on the above research, seven prognostic genes may affect the occurrence and development of glioma by participating in processes such as methylation, cell proliferation, apoptosis, and cell cycle regulation. In addition, the risk model constructed using these seven prognostic genes has been evaluated and verified, and the results show that it has good diagnostic value.

We performed Gene Set Enrichment Analysis (GSEA) on the high-risk and low-risk groups and found that the enrichment was predominantly in pathways such as the biosynthesis of pantothenic acid and coenzyme A, and the generation of IgA within the intestinal immune network, among others. The biosynthesis pathway of pantothenic acid and coenzyme A can provide a large amount of ATP and fatty acids for tumor cells. Meanwhile, it also participates in the acetylation modification process of proteins and the synthesis and activation of some antioxidant enzymes, thus influencing the fate of tumor cells[50]. Some studies have found that there are special IgA antibodies in the outer meninges of mice and humans, and these IgA cells are most similar to the very specific intestinal IgA in the gut, and they share a common origin. This indicates that the brain is protected by intestinal immune cells, and it also directly proves that there is a close connection between the production of IgA in the intestinal immune network and the gut-brain axis[51]. If there is an abnormality in the production of IgA, it may lead to damage to the function of the intestinal mucosal immune barrier, making it easier for pathogens or harmful substances in the intestine to enter the body, triggering a systemic inflammatory response or immune abnormalities. Inflammatory responses and immune abnormalities may affect the

microenvironment of gliomas and indirectly influence the development of gliomas. Our study demonstrated a significant correlation between these pathways and the prognosis of glioma, yet currently, relatively few studies have been involved. The functions of these pathways or related genes and their impacts on the occurrence and development of glioma still need to be elaborated through more research.

Tumor mutation burden is an indicator for evaluating the frequency of gene mutations. When the frequency of gene mutations in tumor cells is high, more tumor antigens are carried on the cell surface, making the cells more susceptible to attacks by the body's immune system[52]. In this study, TCGA mutation data were obtained from TCGA mutations. Based on the analysis of mutation frequencies between the high-risk and low - risk groups, the missense mutation rate of IDH1 was the highest. It was 19% in the high - risk group and 84% in the low-risk group. IDH1 mutations have been frequently mentioned in glioma research. Vorasidenib, a dual inhibitor of mutant IDH1/2, has recently applied for marketing approval in China. Secondly, the mutation rate of TP53 in somatic cells is 41.51%, with a large number of missense mutations. Mutations in the TP53 tumor - suppressor gene are present in approximately 50% of human cancers. As a transcription factor, TP53 directly regulates the expression of about 500 genes, some of which are involved in cell - cycle arrest/cellular senescence, apoptosis, or DNA damage repair, which are cellular responses that jointly prevent tumorigenesis[53]. Some studies have shown that inhibiting the expression of TP53 can induce cancer - like characteristics in human brain organoids, disrupting the cellular structure of the entire organoid[54]. TP53 mutations are also potential prognostic and predictive markers, as well as targets for drug intervention[55]. Mutations or deletions of the TP53 gene are one of the early events in glioma development. Abnormalities of TP53 already exist in some low - grade gliomas, which may make glial cells more prone to malignant transformation, thus initiating tumor formation.

The Tumor Immune Microenvironment (TIME) refers to the complex immune - related internal environment in which tumor cells are located. It has a crucial impact on processes such as tumorigenesis, development, invasion, and metastasis of tumors[56]. There are six immune cells that show significant differences between the high-risk group and the low-risk group. Macrophage M2 is an alternatively activated macrophage. In the tumor microenvironment, macrophage M2 usually exhibits the function of promoting tumor growth and metastasis. The presence of macrophage M2 in the high-risk group may be the reason for its poorer prognosis. The remaining immune cells usually play an anti-tumor role. However, they are not necessarily less abundant in the high-risk group, which may be related to the different immune characteristics between the high-risk group and the low-risk group. Eight immune checkpoints with significant differences were found between the high-risk group and the low-risk group. In addition, we found that the scores of immune-related genes, the status of cancer single cells, the scores of microenvironmental characteristics, and the scores of immunotherapy response were all significantly correlated with the high-risk group. Patients in the high-risk group may obtain greater benefits from immunotherapy than those in the low-risk group. These immune characteristics may affect the occurrence and development of gliomas. Understanding these associations can help develop new immunotherapy strategies to improve the therapeutic effect on the prognosis of gliomas.

By comparing the tumor data of the high-risk group and the low-risk group, we found that there are significant differences between the two groups in terms of the proportion of the immune cycle, the content of immune cells, the expression level of immune checkpoints, and characteristics related to the immune - therapy response. This may be an important reason for the significant difference in prognosis between the two groups.

We utilized the Genomics of Drug Sensitivity in Cancer (GDSC) database to compare the expression differences in the IC50 of common chemotherapeutic drugs between the high - risk group and the low-risk group ($p< 0.05$). The study revealed that Entospletinib and NVP-ADW742 showed the most significant differences. Entospletinib, a spleen tyrosine kinase inhibitor, is used to treat patients with acute myeloid leukemia (AML) who have mutations in tumor protein p53 (TP53) or a complex karyotype. It may inhibit the

growth and proliferation of tumor cells by interfering with relevant cellular signaling pathways through suppressing the activity of Syk[57]. NVP-ADW742 is a novel insulin - like growth factor - I receptor (IGF - IR) kinase inhibitor. Previous studies have indicated that NVP - ADW742 is a highly selective and potent anti - tumor drug, which enhances the chemosensitivity of medulloblastoma cells to temozolomide in vitro[58]. Our research found that these two drugs have a low binding energy with the TP53 gene. Suggesting that they may exert their anti - tumor effects by influencing TP53 - related signaling pathways.

Conclution

In our study, seven ribosome - biogenesis - related prognostic genes with good prognostic value were screened out in gliomas. And they are closely associated with the occurrence and development of gliomas. The risk model constructed based on these seven genes demonstrated a good and stable predictive ability for the prognosis of gliomas. This provides a new theoretical basis and direction for further exploring the common mechanisms by which ribosome biogenesis plays a role in the occurrence and development of gliomas in the future. However, this study did not investigate the specific molecular mechanisms underlying the expression of prognostic genes in gliomas. This awaits further research on our part. In addition, the predictive ability of the prognostic risk model and the clinical practicality of therapeutic drugs still require a large amount of evidence - based medical evidence.

References

1. L. Rong, N. Li, and Z. Zhang, Emerging therapies for glioblastoma: current state and future directions. J Exp Clin Cancer Res 41 (2022) 142.
2. L.R. Schaff, and I.K. Mellinghoff, Glioblastoma and Other Primary Brain Malignancies in Adults: A Review. JAMA 329 (2023) 574-587.
3. S. Grochans, A.M. Cybulska, D. Siminska, J. Korbecki, K. Kojder, D. Chlubek, and I. Baranowska-Bosiacka, Epidemiology of Glioblastoma Multiforme-Literature Review. Cancers (Basel) 14 (2022).
4. J. Pelletier, G. Thomas, and S. Volarevic, Ribosome biogenesis in cancer: new players and therapeutic avenues. Nat Rev Cancer 18 (2018) 51-63.
5. L. Jiao, Y. Liu, X.Y. Yu, X. Pan, Y. Zhang, J. Tu, Y.H. Song, and Y. Li, Ribosome biogenesis in disease: new players and therapeutic targets. Signal Transduct Target Ther 8 (2023) 15.
6. Y. Zang, X. Ran, J. Yuan, H. Wu, Y. Wang, H. Li, H. Teng, and Z. Sun, Genomic hallmarks and therapeutic targets of ribosome biogenesis in cancer. Brief Bioinform 25 (2024).
7. D. Ruggero, and P.P. Pandolfi, Does the ribosome translate cancer? Nat Rev Cancer 3 (2003) 179-92.
8. A.R. Elhamamsy, B.J. Metge, H.A. Alsheikh, L.A. Shevde, and R.S. Samant, Ribosome Biogenesis: A Central Player in Cancer Metastasis and Therapeutic Resistance. Cancer Res 82 (2022) 2344-2353.
9. J. Kang, N. Brajanovski, K.T. Chan, J. Xuan, R.B. Pearson, and E. Sanij, Ribosomal proteins and human diseases: molecular mechanisms and targeted therapy. Signal Transduct Target Ther 6 (2021) 323.
10. Z. Feng, H. Li, N. Chen, K. Xu, and B. Zhang, Deciphering the role of CCL4-CCR5 in coronary artery disease pathogenesis: insights from Mendelian randomization, bulk RNA sequencing, single-cell RNA, and clinical validation. Int J Med Sci 21 (2024) 2683-2693.
11. H.K. Cui, C.J. Tang, Y. Gao, Z.A. Li, J. Zhang, and Y.D. Li, An integrative analysis of single-cell and bulk transcriptome and bidirectional mendelian randomization analysis identified C1Q as a novel stimulated risk gene for Atherosclerosis. Front Immunol 14 (2023) 1289223.
12. Q. He, W. Wang, J. Ma, and G. Consortium, Length of phone use and glioma risk: a Mendelian randomization study. Int J Surg 110 (2024) 5254-5255.
13. S. Zhong, W. Yang, Z. Zhang, Y. Xie, L. Pan, J. Ren, F. Ren, Y. Li, H. Xie, H. Chen, D. Deng, J. Lu, H. Li, B. Wu, Y. Chen, F. Peng, V.K. Puduvalli, K. Sai, Y. Li, Y. Cheng, and Y. Mou, Association between viral infections and glioma risk: a two-sample bidirectional Mendelian randomization analysis. BMC Med 21 (2023) 487.
14. W. Yang, Y. Han, C. He, S. Zhong, F. Ren, Z. Chen, Y. Mou, and K. Sai, Association

between psychiatric disorders and glioma risk: evidence from Mendelian randomization analysis. BMC Cancer 24 (2024) 118.
15. M.E. Ritchie, B. Phipson, D. Wu, Y. Hu, C.W. Law, W. Shi, and G.K. Smyth, limma powers differential expression analyses for RNA-sequencing and microarray studies. Nucleic Acids Res 43 (2015) e47.
16. E.K. Gustavsson, D. Zhang, R.H. Reynolds, S. Garcia-Ruiz, and M. Ryten, ggtranscript: an R package for the visualization and interpretation of transcript isoforms using ggplot2. Bioinformatics 38 (2022) 3844-3846.
17. Z. Gu, R. Eils, and M. Schlesner, Complex heatmaps reveal patterns and correlations in multidimensional genomic data. Bioinformatics 32 (2016) 2847-9.
18. T. Wu, E. Hu, S. Xu, M. Chen, P. Guo, Z. Dai, T. Feng, L. Zhou, W. Tang, L. Zhan, X. Fu, S. Liu, X. Bo, and G. Yu, clusterProfiler 4.0: A universal enrichment tool for interpreting omics data. Innovation (Camb) 2 (2021) 100 141.
19. W. Mao, J. Ding, Y. Li, R. Huang, and B. Wang, Inhibition of cell survival and invasion by Tanshinone IIA via FTH1: A key therapeutic target and biomarker in head and neck squamous cell carcinoma. Exp Ther Med 24 (2022) 521.
20. P. Shannon, A. Markiel, O. Ozier, N.S. Baliga, J.T. Wang, D. Ramage, N. Amin, B. Schwikowski, and T. Ideker, Cytoscape: a software environment for integrated models of biomolecular interaction networks. Genome Res 13 (2003) 2498-504.
21. G. Hemani, J. Zheng, B. Elsworth, K.H. Wade, V. Haberland, D. Baird, C. Laurin, S. Burgess, J. Bowden, R. Langdon, V.Y. Tan, J. Yarmolinsky, H.A. Shihab, N.J. Timpson, D.M. Evans, C. Relton, R.M. Martin, G. Davey Smith, T.R. Gaunt, and P.C. Haycock, The MR-Base platform supports systematic causal inference across the human phenome. Elife 7 (2018).
22. J. Bowden, G. Davey Smith, and S. Burgess, Mendelian randomization with invalid instruments: effect estimation and bias detection through Egger regression. Int J Epidemiol 44 (2015) 512-25.
23. J. Bowden, G. Davey Smith, P.C. Haycock, and S. Burgess, Consistent Estimation in Mendelian Randomization with Some Invalid Instruments Using a Weighted Median Estimator. Genet Epidemiol 40 (2016) 304-14.
24. S. Burgess, R.A. Scott, N.J. Timpson, G. Davey Smith, S.G. Thompson, and E.-I. Consortium, Using published data in Mendelian randomization: a blueprint for efficient identification of causal risk factors. Eur J Epidemiol 30 (2015) 543-52.
25. F.P. Hartwig, G. Davey Smith, and J. Bowden, Robust inference in summary data Mendelian randomization via the zero modal pleiotropy assumption. Int J Epidemiol 46 (2017) 1985-1998.
26. P. Zhao, H. Zhen, H. Zhao, Y. Huang, and B. Cao, Identification of hub genes and potential molecular mechanisms related to radiotherapy sensitivity in rectal cancer based on multiple datasets. J Transl Med 21 (2023) 176.
27. Y. Fang, S. Huang, L. Han, S. Wang, and B. Xiong, Comprehensive Analysis of Peritoneal Metastasis Sequencing Data to Identify LINC00924 as a Prognostic Biomarker in Gastric Cancer. Cancer Manag Res 13 (2021) 5599-5611.
28. J. Friedman, T. Hastie, and R. Tibshirani, Regularization Paths for Generalized Linear Models via Coordinate Descent. J Stat Softw 33 (2010) 1-22.
29. T.T. Liu, R. Li, C. Huo, J.P. Li, J. Yao, X.L. Ji, and Y.Q. Qu, Identification of CDK2-Related Immune Forecast Model and ceRNA in Lung Adenocarcinoma, a Pan-Cancer Analysis. Front Cell Dev Biol 9 (2021) 682002.
30. P.J. Heagerty, T. Lumley, and M.S. Pepe, Time-dependent ROC curves for censored survival data and a diagnostic marker. Biometrics 56 (2000) 337-44.
31. M.I. Love, W. Huber, and S. Anders, Moderated estimation of fold change and dispersion for RNA-seq data with DESeq2. Genome Biol 15 (2014) 550.
32. G. Yu, Gene Ontology Semantic Similarity Analysis Using GOSemSim. Methods Mol Biol 2117 (2020) 207-215.
33. S. Orifjon, J. Jammatov, C. Sousa, R. Barros, O. Vasconcelos, and P. Rodrigues, Translation and Adaptation of the Adult Developmental Coordination Disorder/Dyspraxia Checklist (ADC) into Asian Uzbekistan. Sports (Basel) 11 (2023).
34. K. Ellrott, M.H. Bailey, G. Saksena, K.R. Covington, C. Kandoth, C. Stewart, J. Hess, S.

Ma, K.E. Chiotti, M. McLellan, H.J. Sofia, C. Hutter, G. Getz, D. Wheeler, L. Ding, M.C.W. Group, and N. Cancer Genome Atlas Research, Scalable Open Science Approach for Mutation Calling of Tumor Exomes Using Multiple Genomic Pipelines. Cell Syst 6 (2018) 271-281 e7.
35. A. Mayakonda, D.C. Lin, Y. Assenov, C. Plass, and H.P. Koeffler, Maftools: efficient and comprehensive analysis of somatic variants in cancer. Genome Res 28 (2018) 1747-1756.
36. S. Hanzelmann, R. Castelo, and J. Guinney, GSVA: gene set variation analysis for microarray and RNA-seq data. BMC Bioinformatics 14 (2013) 7.
37. L. Yang, Y.H. Shou, Y.S. Yang, and J.H. Xu, Elucidating the immune infiltration in acne and its comparison with rosacea by integrated bioinformatics analysis. PLoS One 16 (2021) e0248650.
38. W. Zhang, R. Dang, H. Liu, L. Dai, H. Liu, A.A. Adegboro, Y. Zhang, W. Li, K. Peng, J. Hong, and X. Li, Machine learning-based investigation of regulated cell death for predicting prognosis and immunotherapy response in glioma patients. Sci Rep 14 (2024) 4173.
39. D. Maeser, R.F. Gruener, and R.S. Huang, oncoPredict: an R package for predicting in vivo or cancer patient drug response and biomarkers from cell line screening data. Brief Bioinform 22 (2021).
40. L. Kong, Y. Xiong, D. Wang, L. Huang, M. Li, Z. Feng, Y. Zhou, H. Zhang, F. Liu, F. Xiao, Y. Wei, and W. Zhang, Intermedin (adrenomedullin 2) promotes breast cancer metastasis via Src/c-Myc-mediated ribosome production and protein translation. Breast Cancer Res Treat 195 (2022) 91-103.
41. L. Yang, K. Niu, J. Wang, W. Shen, R. Jiang, L. Liu, W. Song, X. Wang, X. Zhang, R. Zhang, D. Wei, M. Fan, L. Jia, and K. Tao, Nucleolin lactylation contributes to intrahepatic cholangiocarcinoma pathogenesis via RNA splicing regulation of MADD. J Hepatol 81 (2024) 651-666.
42. Y. Cheng, G. Zhao, S. Zhang, F. Nigim, G. Zhou, Z. Yu, Y. Song, Y. Chen, and Y. Li, AS1411-Induced Growth Inhibition of Glioma Cells by Up-Regulation of p53 and Down-Regulation of Bcl-2 and Akt1 via Nucleolin. PLoS One 11 (2016) e0167094.
43. W. Tao, H. Lei, W. Luo, Z. Huang, P. Ling, M. Guo, L. Wan, K. Zhai, Q. Huang, Q. Wu, S. Xu, L. Zeng, X. Wang, Z. Dong, J.N. Rich, and S. Bao, Novel INHAT repressor drives glioblastoma growth by promoting ribosomal DNA transcription in glioma stem cells. Neuro Oncol 25 (2023) 1428-1440.
44. D. Zhang, B. Li, H. Xu, J. Li, C. Ma, W. Ge, C. Lu, and X. Cao, Identification of FBLL1 as a neuron-specific RNA 2'-O-methyltransferase mediating neuronal differentiation. Proc Natl Acad Sci U S A 121 (2024) e2406961121.
45. B. Zhang, M.Y. Chen, Y.J. Shen, X.B. Zhuo, P. Gao, F.S. Zhou, B. Liang, J. Zu, Q. Zhang, S. Suleman, Y.H. Xu, M.G. Xu, J.K. Xu, C.C. Liu, N. Giannareas, J.H. Xia, Y. Zhao, Z.L. Huang, Z. Yang, H.D. Cheng, N. Li, Y.Y. Hong, W. Li, M.J. Zhang, K.D. Yu, G. Li, M.H. Sun, Z.D. Chen, G.H. Wei, and Z.M. Shao, A Large-Scale, Exome-Wide Association Study of Han Chinese Women Identifies Three Novel Loci Predisposing to Breast Cancer. Cancer Res 78 (2018) 3087-3097.
46. Y.H. Kim, S. Nobusawa, M. Mittelbronn, W. Paulus, B. Brokinkel, K. Keyvani, U. Sure, K. Wrede, Y. Nakazato, Y. Tanaka, A. Vital, L. Mariani, R. Stawski, T. Watanabe, U. De Girolami, P. Kleihues, and H. Ohgaki, Molecular classification of low-grade diffuse gliomas. Am J Pathol 177 (2010) 2708-14.
47. R. Keener, S.B. Chhetri, C.J. Connelly, M.A. Taub, M.P. Conomos, J. Weinstock, B. Ni, B. Strober, S. Aslibekyan, P.L. Auer, L. Barwick, L.C. Becker, J. Blangero, E.R. Bleecker, J.A. Brody, B.E. Cade, J.C. Celedon, Y.C. Chang, L.A. Cupples, B. Custer, B.I. Freedman, M.T. Gladwin, S.R. Heckbert, L. Hou, M.R. Irvin, C.R. Isasi, J.M. Johnsen, E.E. Kenny, C. Kooperberg, R.L. Minster, T. Naseri, S. Viali, S. Nekhai, N. Pankratz, P.A. Peyser, K.D. Taylor, M.J. Telen, B. Wu, L.R. Yanek, I.V. Yang, C. Albert, D.K. Arnett, A.E. Ashley-Koch, K.C. Barnes, J.C. Bis, T.W. Blackwell, E. Boerwinkle, E.G. Burchard, A.P. Carson, Z. Chen, Y.I. Chen, D. Darbar, M. de Andrade, P.T. Ellinor, M. Fornage, B.D. Gelb, F.D. Gilliland, J. He, T. Islam, S. Kaab, S.L.R. Kardia, S. Kelly, B.A. Konkle, R. Kumar, R.J.F. Loos, F.D. Martinez, S.T. McGarvey, D.A. Meyers, B.D. Mitchell, C.G.

Montgomery, K.E. North, N.D. Palmer, J.M. Peralta, B.A. Raby, S. Redline, S.S. Rich, D. Roden, J.I. Rotter, I. Ruczinski, D. Schwartz, F. Sciurba, M.B. Shoemaker, E.K. Silverman, M.F. Sinner, N.L. Smith, A.V. Smith, H.K. Tiwari, R.S. Vasan, S.T. Weiss, L.K. Williams, Y. Zhang, E. Ziv, L.M. Raffield, A.P. Reiner, N.T.-O.f.P.M. Consortium, T.O. Hematology, G. Hemostasis Working, T.O.S.V.W. Group, M. Arvanitis, C.W. Greider, et al., Validation of human telomere length multi-ancestry meta-analysis association signals identifies POP5 and KBTBD6 as human telomere length regulation genes. Nat Commun 15 (2024) 4417.

48. Y. Dong, Q. Cai, L. Fu, H. Liu, M. Ma, and X. Wu, Study of the G Protein Nucleolar 2 Value in Liver Hepatocellular Carcinoma Treatment and Prognosis. Biomed Res Int 2021 (2021) 4873678.
49. Q. Li, C. Ye, T. Tian, Q. Jiang, P. Zhao, X. Wang, F. Liu, J. Shan, and J. Ruan, The emerging role of ubiquitin-specific protease 20 in tumorigenesis and cancer therapeutics. Cell Death Dis 13 (2022) 434.
50. P. Kreuzaler, P. Inglese, A. Ghanate, E. Gjelaj, V. Wu, Y. Panina, A. Mendez-Lucas, C. MacLachlan, N. Patani, C.B. Hubert, H. Huang, G. Greenidge, O.M. Rueda, A.J. Taylor, E. Karali, E. Kazanc, A. Spicer, A. Dexter, W. Lin, D. Thompson, M. Silva Dos Santos, E. Calvani, N. Legrave, J.K. Ellis, W. Greenwood, M. Green, E. Nye, E. Still, C.R.G.C. Consortium, S. Barry, R.J.A. Goodwin, A. Bruna, C. Caldas, J. MacRae, L.P.S. de Carvalho, G. Poulogiannis, G. McMahon, Z. Takats, J. Bunch, and M. Yuneva, Vitamin B(5) supports MYC oncogenic metabolism and tumor progression in breast cancer. Nat Metab 5 (2023) 1870-1886.
51. Z. Fitzpatrick, G. Frazer, A. Ferro, S. Clare, N. Bouladoux, J. Ferdinand, Z.K. Tuong, M.L. Negro-Demontel, N. Kumar, O. Suchanek, T. Tajsic, K. Harcourt, K. Scott, R. Bashford-Rogers, A. Helmy, D.S. Reich, Y. Belkaid, T.D. Lawley, D.B. McGavern, and M.R. Clatworthy, Gut-educated IgA plasma cells defend the meningeal venous sinuses. Nature 587 (2020) 472-476.
52. J. Budczies, D. Kazdal, M. Menzel, S. Beck, K. Kluck, C. Altburger, C. Schwab, M. Allgauer, A. Ahadova, M. Kloor, P. Schirmacher, S. Peters, A. Kramer, P. Christopoulos, and A. Stenzinger, Tumour mutational burden: clinical utility, challenges and emerging improvements. Nat Rev Clin Oncol 21 (2024) 725-742.
53. Z. Wang, A. Strasser, and G.L. Kelly, Should mutant TP53 be targeted for cancer therapy? Cell Death Differ 29 (2022) 911-920.
54. S.K. Singh, Y. Wang, A. Habib, M. Priyadarshini, C.V. Kodavali, A. Chen, W. Ma, J. Wang, N.U.F. Hameed, B. Hu, G.N. Fuller, S.M. Kulich, N. Amankulor, R.R. Colen, L.A. Edwards, and P.O. Zinn, TP53-PTEN-NF1 depletion in human brain organoids produces a glioma phenotype in vitro. Front Oncol 13 (2023) 1279806.
55. M. Olivier, M. Hollstein, and P. Hainaut, TP53 mutations in human cancers: origins, consequences, and clinical use. Cold Spring Harb Perspect Biol 2 (2010) a001008.
56. M. Zhu, Y. Hu, Y. Gu, X. Lin, X. Jiang, C. Gong, and Z. Fang, Role of amino acid metabolism in tumor immune microenvironment of colorectal cancer. Am J Cancer Res 15 (2025) 233-247.
57. V.H. Duong, A.S. Ruppert, A.S. Mims, U. Borate, E.M. Stein, M.R. Baer, W. Stock, T. Kovacsovics, W. Blum, M.L. Arellano, G.J. Schiller, R.L. Olin, J.M. Foran, M.R. Litzow, T.L. Lin, P.A. Patel, M.C. Foster, R.L. Redner, Z. Al-Mansour, C.R. Cogle, R.T. Swords, R.H. Collins, J.A. Vergilio, N.A. Heerema, L. Rosenberg, A.O. Yocum, S. Marcus, T. Chen, F. Druggan, M. Stefanos, T.J. Gana, A.B. Shoben, B.J. Druker, A. Burd, J.C. Byrd, R.L. Levine, and M.M. Boyiadzis, Entospletinib with decitabine in acute myeloid leukemia with mutant TP53 or complex karyotype: A phase 2 substudy of the Beat AML Master Trial. Cancer 129 (2023) 2308-2320.
58. H. Zhou, J. Rao, J. Lin, B. Yin, H. Sheng, F. Lin, N. Zhang, and L. Yang, The insulin-like growth factor-I receptor kinase inhibitor NVP-ADW742 sensitizes medulloblastoma to the effects of chemotherapy. Oncol Rep 25 (2011) 1565-71.